metals

MDPI

Article

On the Improvement of AA2024 Wear Properties through the Deposition of a Cold-Sprayed Titanium Coating

Antonello Astarita [1,*], Felice Rubino [2], Pierpaolo Carlone [2], Alessandro Ruggiero [2], Claudio Leone [3,4], Silvio Genna [4], Massimiliano Merola [2] and Antonino Squillace [1]

[1] Department of Chemical, Materials and Industrial Production Engineering, University of Naples Federico II, P. Tecchio 80, Naples 80125, Italy; squillac@unina.it
[2] Department of Industrial Engineering, University of Salerno, Via Giovanni Paolo II, Fisciano, Salerno 84084, Italy; frubino@unisa.it (F.R.); pcarlone@unisa.it (P.C.); ruggiero@unisa.it (A.R.); mmerola@unisa.it (M.M.)
[3] Department of Industrial and Information Engineering, Second University of Naples, Via Roma 29, Aversa (Ce) 81031, Italy; claudio.leone@unina.it
[4] CIRTIBS Research Centre, University of Naples Federico II, P.le Tecchio 80, Naples 80125, Italy; sgenna@unina.it
* Correspondence: antonello.astarita@unina.it; Tel.: +39-081-768-2364

Academic Editor: Nong Gao
Received: 25 March 2016; Accepted: 4 August 2016; Published: 11 August 2016

Abstract: This paper deals with the study of the enhancement of the tribological properties of AA2024 through the deposition of a titanium coating. In particular two different coatings were studied: (1) untreated titanium coating; and (2) post-deposition laser-treated titanium coating. Titanium grade 2 powders were deposited onto an aluminium alloy AA2024-T3 sheet through the cold gas dynamic spray process. The selective laser post treatment was carried out by using a 220 W diode laser to further enhance the wear properties of the coating. Tribo-tests were executed to analyse the tribological behaviour of materials in contact with an alternative moving counterpart under a controlled normal load. Four different samples were tested to assess the effectiveness of the treatments: untreated aluminium sheets, titanium grade 2 sheets, as-sprayed titanium powders and the laser-treated coating layer. The results obtained proved the effectiveness of the coating in improving the tribological behaviour of the AA2024. In particular the laser-treated coating showed the best results in terms of both the friction coefficient and mass lost. The laser treatment promotes a change of the wear mechanism, switching from a severe adhesive wear, resulting in galling, to an abrasive wear mechanism.

Keywords: AA 2024; titanium; cold spray; laser treating; coating; wear; tribotest

1. Introduction

Aluminium alloys are widely used in many industrial fields (e.g., aerospace, automotive, naval, buildings and so on) due to their low weight, ease of manufacturing and good mechanical and electrochemical properties. On the other hand, for some applications (e.g., coupling with carbon fibre-reinforced plastics, applications in high corrosive environments or applications in which a superior wear resistance is required) enhanced superficial properties, in terms of both corrosion resistance and wear resistance, are required. A solution that could overcome these issues is the production of titanium coatings on aluminium components. In this way it is possible to couple the light weight and relatively low-cost nature of aluminium with the high superficial properties of titanium.

This solution is of particular interest in aeronautics, in which light weight is a primary requirement for all the components.

Aluminium alloys mainly used in aeronautics, e.g., the alloys of 2xxx and 7xxx series, are heat-treatable alloys and are age hardened. Thus, they require a deposition technique in which the substrate remains at a low temperature during the whole process. Cold gas dynamic spray (CGDS) is an innovative deposition technology matching these requirements. CGDS is an additive manufacturing process used to create a coating layer by means of high velocity impacts of metallic particles dispersed in supersonic gas flows. In this process, coating deposition occurs at relatively low temperatures when compared to other spray technologies, allowing sprayed particles to preserve their solid state. Appropriate flow conditions are enforced, combining a high pressure-heated gas with a converging/diverging nozzle (De Laval nozzle). Metallic particles are propelled to supersonic velocity (i.e., 500–1000 m/s), and the high kinetic energy causes the impingement of the particles onto the substrate [1]. The macroscopic plastic deformation, induced by the high velocity impact, was indicated by some researchers as the main bonding mechanism [2,3]. Two different scenarios have been observed, depending on material pairing and particle velocity: (a) particles rebounding from the substrate or (b) particles bonding to the substrate [4]. The velocity at which bonding is achieved is referred to as the critical velocity and relies on the particle size and distribution as well as the substrate material. The coatings exhibit high density and conductivity, good corrosion resistance and high hardness, due to the cold worked microstructure [5]. Recent studies discussed the capabilities of post-deposition laser treatments to compensate for some process drawbacks, reducing the porosity, improving the superficial hardness and increasing the anti-corrosion and tribological properties of the coating [6–8]. Several post-deposition treatments were successfully used to modify the microstructure and to improve the properties of the cold-sprayed titanium layer. Marrocco et al. (2011) proved that post-deposition laser treatment on titanium coating eliminates the residual micro-porosity and forms a high quality corrosion barrier layer [3]. Other authors studied the laser treatments in order to improve the superficial properties of both coatings and bulk materials [9–11]. The authors' previous work showed the optimal process parameters of the laser treatment to obtain a compact titanium dioxide layer on cold-sprayed titanium coating [12]. In literature, other authors investigated the deposition of titanium coatings in order to improve the tribological properties [13,14], where different coating techniques were taken into account.

This paper presents a study of the enhancement of the wear properties of an AA2024 rolled sheet through the deposition of a cold-sprayed titanium coating.

Two different coatings were studied, (1) untreated coating; (2) post-deposition laser-treated coating, in order to assess the influence of the laser treatment on the wear and tribological properties of titanium cold spray coating. Current developments in Ti processing predict the accessibility of lower-cost Ti and have revived interests in exploring the tribo-behaviour of Ti alloys as bearing materials [15–18]. Titanium and its alloys exhibit low tribological properties but their wear resistance can be improved by surface treatments promoting growth of the surface hardness, leading to changes of the wear mechanism and a lowering of the wear rate [19]. Frictional contact of titanium alloys both against other materials and titanium alloys themselves, especially under pure sliding conditions, quickly damages the contact surface area and results in the transfer of some particles of the material to the counter face [20,21]. Titanium and its alloys are characterised by a high and unstable friction factor and strong adhesive wear degradation through an elevated propensity to seizure (localised damage due to the diffusion welding between sliding surfaces [22]) and scuffing (damage characterised by surface unevenness and asperities called hillocks [23]). A couple of papers dealing with the tribological properties of cold-sprayed titanium coatings [24,25] are also available in the literature, but, to date, the coupling between the cold-sprayed coating and laser treatment has not been studied and understood.

Tribological characteristics of titanium alloys can be improved by different kinds of treatments. Cassar et al. [26] proposed a triode plasma oxidation treatment on Ti-6Al-4V, finding a reduction in the wear rate under a range of different wear test regimes. Wang et al. [27] studied the time-dependant effects of thermal oxidation in aqueous atmospheres performed on Ti-6Al-4V alloy which affect its surface roughness and wear properties. The fretting tests performed revealed an improvement in the fretting wear resistance after oxidation and an optimum time treatment equal to 4 h. Bell and Dong (2000) [6] proved that the oxidation treatment of Ti6Al4V led to a significant improvement in wear resistance, but there is no detailed analysis focusing on the application of the laser treatments on cold-sprayed coatings. Friction and wear tests were performed on untreated aluminium sheets, titanium grade 2 sheets, as-sprayed titanium powders and the laser-treated coating layer to compare the wear properties of different materials and investigate the effectiveness of the treatments.

2. Experimental Section

Commercially pure grade 2 titanium particles with a mean size of approximately 40 μm were deposited onto 3-mm-thick AA2024-T3 plates. The chemical composition and the main properties of both grade 2 titanium and AA2024 are available in literature [28,29] and not here reported in the interest of brevity. A low pressure cold spray facility equipped with a round-shaped exit nozzle, with a final diameter of 4.8 mm, was used for spraying. Helium, used as carrier gas, avoided the oxidation of titanium particles during the deposition process. The particles were sprayed at a velocity of 680 m/s with helium as carrier gas, the gas temperature and pressure were kept at 600 °C and at 12 bars. A superficial layer of cold sprayed titanium powder 5 mm thick was obtained. The successive milling process allowed to obtain the surface finishing required for the following laser treatment and tribo-tests. After the milling process, a 2.5-mm-thick titanium coating with a good superficial finishing was obtained. Laser treatments were carried out using a diode laser (IPG DLR-200-AC, IPG Photonics, Tokyo, Japan). The laser power is transferred via an optical fibre to the laser head and focused/defocused on the plate surface by means of a focusing lens (corresponding to a spot diameter of about 2 mm). Previous work [12] gave necessary information about optimal process parameters to obtain a fully dense and compact titanium oxidised layer on cold-sprayed coating surface: scan speed and power of laser beam were 50 mm/min and 200 W.

Friction and wear tests were performed with a ball-on-flat testing apparatus on a TR-BIO 282 Reciprocatory Friction Monitor (Ducom Instruments, Bangalore, India), following a consolidate protocol [30,31]. The tribopair was made up by a titanium ball and a flat specimen of the analysed materials, aluminium alloy, titanium grade 2, titanium as-sprayed coating and laser treated layer. The Ti6Al4V ball had a diameter of 3 mm, the specimens were realised with dimensions of $25 \times 25 \times 5$ mm^3. The reciprocating movement was imposed to the sphere by a stepper motor. The frictional force was monitored by a load cell, and the evolution of the coefficient of friction, during the test, was recorded. A gravimetric analysis was accomplished to evaluate the wear, expressed as mass loss. Before each test, the sample and the ball were cleaned with ethanol and compressed air, subsequently weighted on a precision scale (accuracy of 0.01 mg). These tests were made in partial compliance with the prescriptions of Test Method ASTM G133, Procedure A. The normal force was 12.0 N, instead of 25.0 N, and the test time was 20 min, instead of 16 min and 40 s as prescribed by the norm. All other advices of Test Method G133 were followed: the stroke length and the frequency oscillation were respectively 10 mm and 5 Hz (alternative motion). Considering the smaller radius of the ball—1.5 mm instead of the 4.7 mm radius recommended—a lower load was applied, the resulting pressure (Hertzian contact stress) was around 1.4 GPa, which is a suitable stress for such tribocouples. A longer test was required to look for a stable value of the friction coefficient, this choice brought a total sliding distance of 120 m instead of 100 m. Every test was realised at room temperature, in laboratory air at controlled levels of relative humidity. A topographic surface acquisition was carried out with a 3D non-contact optical profilometer, PLμ neox (Sensofar, Terrassa, Spain), which operates either as a confocal microscope or as a white light interferometer. The worn surfaces, previously cleaned from debris, were scanned using a confocal lens with magnification of 5×. The scans provided 3D and contour images, which gave qualitative information on the wear process and quantitative information, such as the maximum wear depth.

Microscopical analysis were also performed, employing Scanning Electron Microscopy (Hitachi TM 3000, Tokyo, Japan), to observe macroscopic features (depth and width) of the laser treated zone as well as to investigate microstructural aspects. Kroll's reagent (2 mL HF, 6 mL HNO_3 and H_2O up to 100 mL) was adopted to unveil microstructure, grain boundaries and phase distribution. Finally, Vickers microhardness tests were conducted on the laser treated specimen to characterise the mechanical properties of material.

3. Results and Discussion

Micrographies of a laser treated specimen (Figure 1) show a dense titanium oxide layer produced on the surface of the titanium coating. In the centre of the treated sample the oxide penetrates the coating up to about 30% of its thickness. Below the oxide layer, the heat produced by the laser source caused the formation a heat-affected zone, characterised by a microstructure with a coarser grain than the material base. In the discussion, the following terms will be used to identify the different metallurgical zones:

(1) Oxidised zone: the region of the cold-sprayed layer that was oxidised by the laser treatment;
(2) Heat-affected zone: similarly to what happens in laser beam welding, this is the region of the cold-sprayed layer that was affected by the heat generated during the treatment;
(3) Base material: the region of the cold-sprayed layer that was not affected by the laser treatment;
(4) Substrate: the aluminium plate used as a substrate for the deposition process.

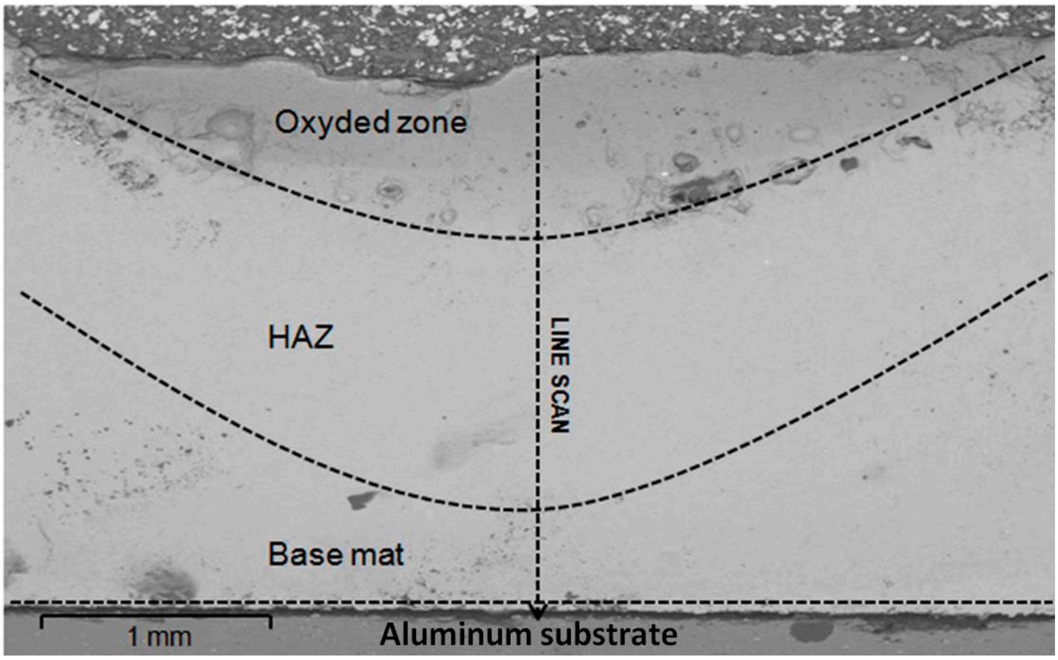

Figure 1. Cross-section of laser treated specimen (magnification 60×).

Figure 2 shows the different microstructures produced by the laser treatment within the cold-sprayed layer. Three different zones are visible in the sections of the treated specimen: the oxidised zone (Figure 2a), in which the typical microstructure of the titanium oxide is exhibited, the heat-affected zone (Figure 2b), which is characterised by lamellae of coarser dimensions than the as-sprayed titanium due to the heat input occurring during the laser process, and the base material (Figure 2c), characterised by lamellae of coarser dimensions. EDS analyses confirmed the existence of a rutile (TiO_2

titanium dioxide) layer. Line scan EDS analysis (Figure 3), performed in the center of the cross-section following the pattern labelled "line scan" represented in Figure 1, revealed the concentration of titanium and oxygen from the top of the surface to the interface between the coating and substrate.

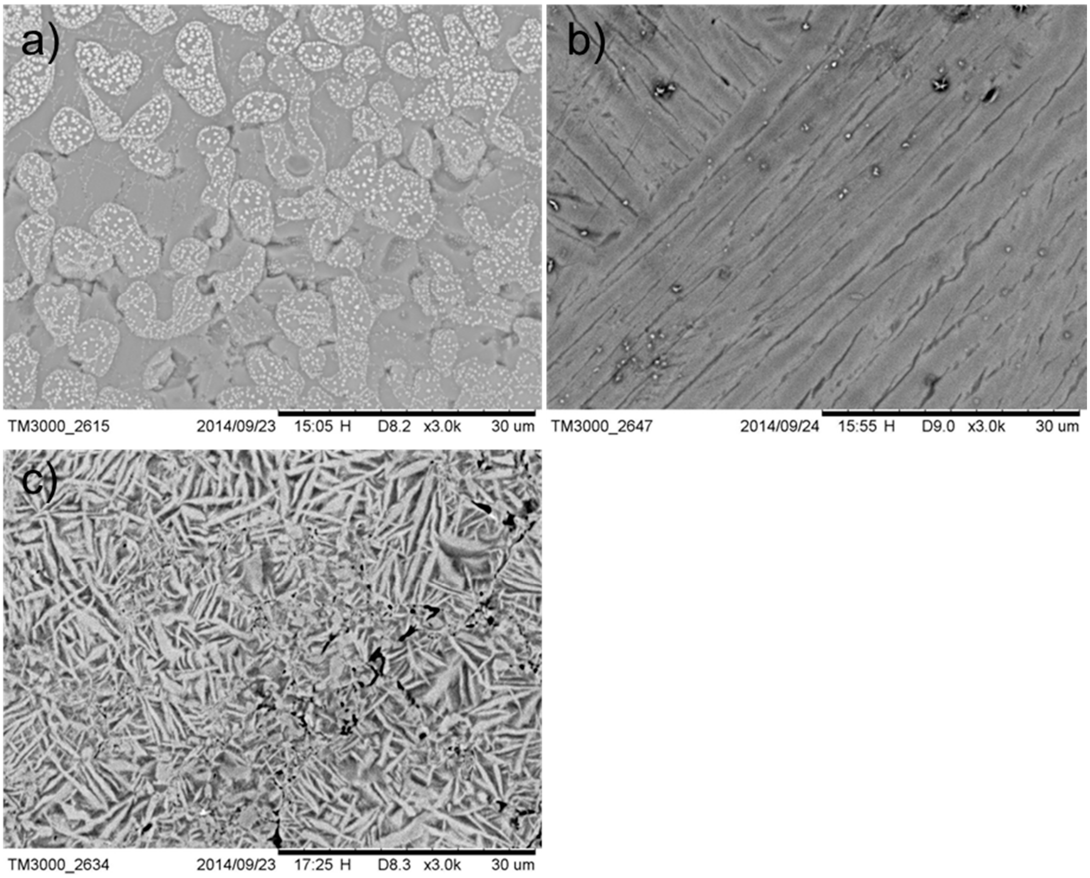

Figure 2. Different microstructures observed in the cold-sprayed coating after the laser treatment: (**a**) titanium oxidised zone; (**b**) heat-affected zone; (**c**) base material.

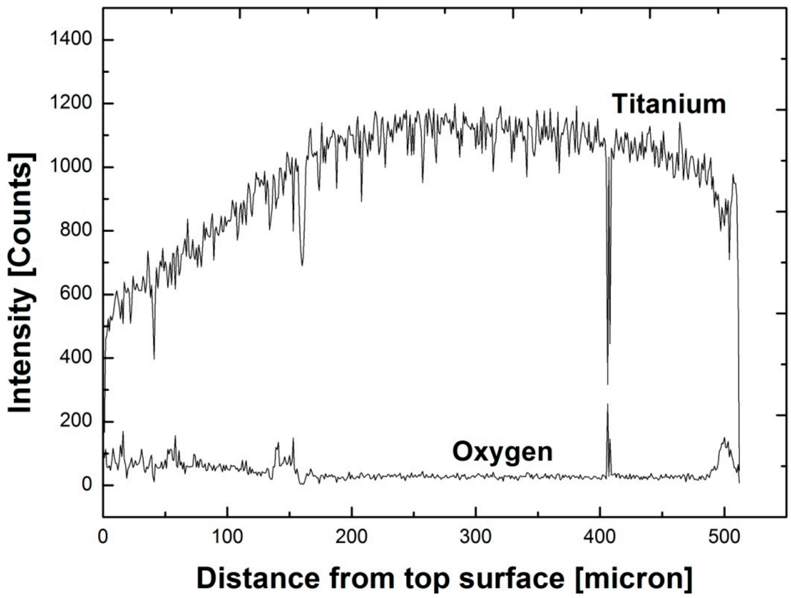

Figure 3. Titanium and oxygen intensity along the scan line indicated in Figure 1.

The relative concentration of two elements (Ti, O), in the topmost layer of the cross-section, is approximately equal to the stoichiometric one for the titanium dioxide; moving to the interface with the aluminium substrate, the oxygen percentage decreases to characteristic values of titanium grade 2. It should be noted that the XRD analysis of the treated surface, presented by the authors in a previous paper [32], confirmed the formation of a rutile layer as well as a thick oxygen diffused zone underlying the oxidised zone. This result will be useful in the further discussion of the results.

The micro-hardness values of treated materials on the coating surface were about 1000 HV, much greater than the values of cold-sprayed titanium (about 200 HV) reported in the literature [33] (Figure 4). The tests were performed following the same pattern of the EDS analysis.

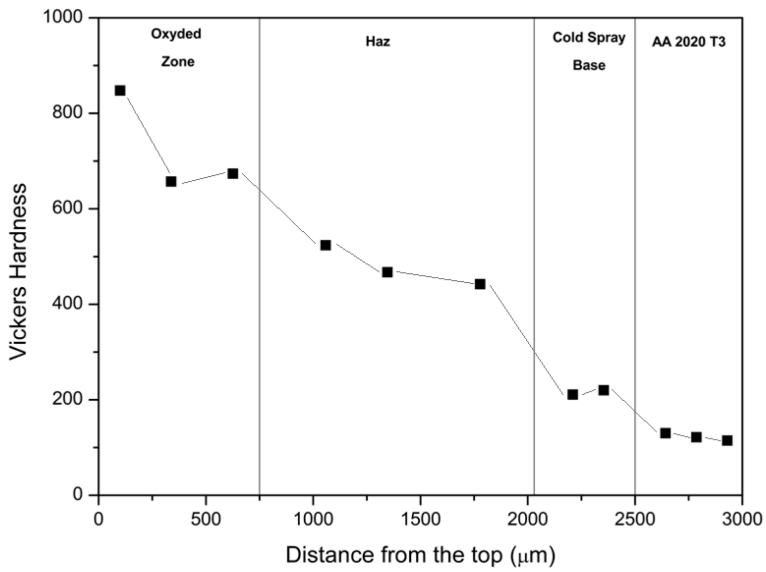

Figure 4. Microhardness measurements taken through the plate cross-section.

Microhardness measurements strongly indicated the formation of a very hard surface layer. This observation is in agreement with the results of the tribological test (Figure 2), which showed the major mass loss occurred in the titanium ball rather than in the laser-treated titanium. In addition, microhardness tests on the substrate indicated a microhardness close to 150 HV (the pre-deposition microhardness of the AA 2024 T3 alloy) which suggests that the aluminium substrate was mechanically unaffected by the deposition process. Thus, it can be conjectured that both the deposition process and the laser treatment do not affect the temper state of the aluminium substrate, which is an extremely important result of this work.

The main aim of the tribo-tests was to evaluate the wear resistance of the materials. Tribological tests have highlighted that the laser treatment can significantly improve the friction and wear properties of titanium. Figure 5 compares the development of the friction coefficient (CoF) of the laser-treated coating with the cold-sprayed coating, as well as samples of the as-received titanium and aluminium alloy.

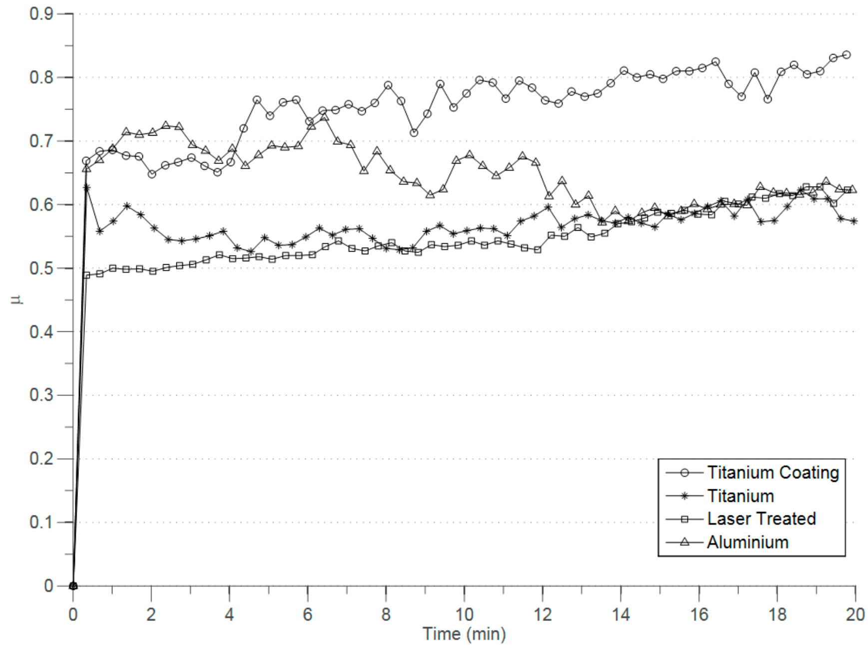

Figure 5. Evolution of friction coefficients for the processed plates with time.

The evolution of the friction coefficient is unsteady and its variation derives from two elements: the trend and the fluctuations around the mean value. The trend is due to several phenomena such as the reciprocal adjustment of surface asperities leading to an alteration of the real contact area, the inclusion of (micro) wear debris [34]—third body wear—and the variability of the contact temperature; the fluctuation around the mean is typical of the reciprocating test where the relative velocity is variable. The aluminium plate vs. titanium ball tribopair couple (the latter, hereinafter, omitted for simplicity) indicates a slightly increasing trend only after 14 min of testing, where μ is near 0.60. For the titanium plate μ was in the range of 0.50–0.60 for the duration of the test, ending with a constant trend. This result is consistent with the values proposed by Miller and Budinski [35,36], who, in their investigations on the tribological properties of titanium and its alloys, analysed several tribo-pairings and wear mechanisms. In the case of the titanium cold spray coating, after 14 min, fluctuations were still noticeable due to the surface unevenness (a characteristic of the as-sprayed coating) and the friction coefficient, μ, varied in the range of 0.75–0.85, with an increasing trend. This trend is consistent with the results of Khun et al. [25]. They observed a higher friction coefficient of Ti cold spray coating compared to the Ti bulk material, with a very irregular profile and large fluctuations. The measured value CoF, after an initial peak, reached a steady-state value of approximately 0.78. Finally, the development of the laser-treated coating presented a rising trend, reaching—with small fluctuations—the value of 0.62. The overall rising trend in the final phase of the tests is supported by the results of Wang et al. from their tribological analysis on rutile coating [27], where the formation of debris is held accountable for this phenomenon. From our analysis a similar behaviour emerged from the different tribocouples in the last six minutes of the test, excluding the titanium coating for which higher μ values were found. In Figure 6, the results from the gravimetric analysis are presented. Both the values of the specimen wear and the sphere wear are shown and summed up. Concerning the aluminium case, the wear of the ball was almost zero, whereas the flat sample lost a considerable quantity of mass. Laser-treated coating returned the highest wear of the ball with respect to the different tribopairs. On the other hand, this specimen lost very little mass. The overall wear of the tribopair for the laser-treated coating case is comparable to the one relative to the titanium plate; in the latter case, however, the main loss was detected on the specimen side. The oxidation of titanium indicated significant improvements in its tribological properties. The TiO_2 showed a smoother friction coefficient profile with less fluctuations and reached a lower value of μ compared to the titanium plate, which is characterised by an unstable CoF with evident fluctuations. The same behaviour was observed for the cold spray coating. The improvements are also highlighted by the limited wear rate of the oxidised coating (see Figure 6), which is much lower than the as-sprayed titanium and titanium bulk material. Krishna et al. [37] confirmed this behaviour. They proposed that the improvement in wear resistance is due to the high hardness of the oxide layer and its strong adhesion with the underlying material. Dalili et al. [38] confirmed the role played by the enhanced surface hardness, resulting from the formation of a harder oxide layer and a thick oxygen diffusion zone, in improving the wear resistance of titanium which resulted in a lower friction coefficient and negligible weight loss. They proposed that the oxide layer prevents extensive plastic deformation of the titanium, thus changing the nature of the contact area from metallic/metallic pair to ceramic/metallic tribo-pair [39,40]. This improvement of the wear properties of the titanium layer is fundamentally linked to the presence and contribution of rutile. In this regard, in his papers [41] on the tribological properties of titanium, Sun proved that the improvement of the tribological properties of the titanium after the thermal oxidation treatment can be attributed to the formation of a rutile layer and also highlighted the correlation between the tribological properties and the characteristics of the rutile [42].

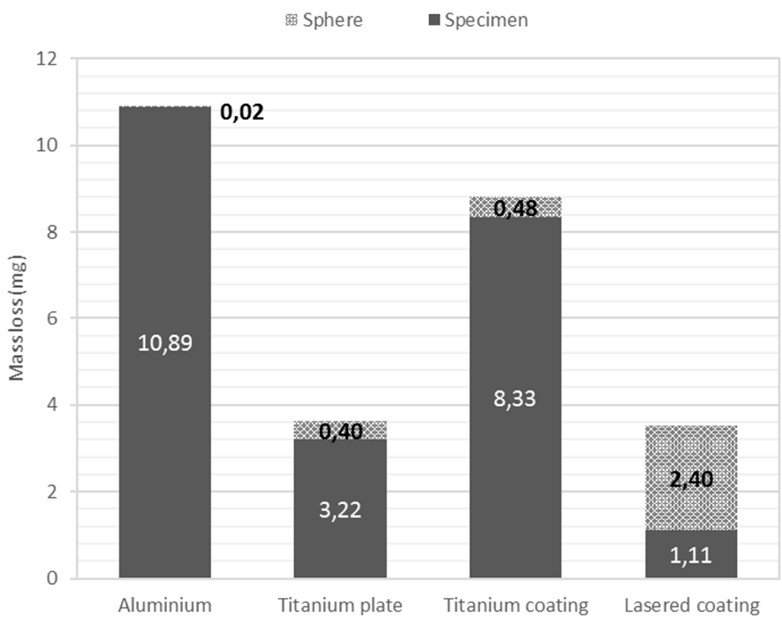

Figure 6. Wear comparison in term of mass loss for the four processing methods.

The tribotest instrument recorded the evolution of the frictional force during the sliding of the sphere along the test, and the force was recorded with an acquisition frequency equal to 100 times the oscillating frequency.

In Figure 7, the typical evolution of the frictional force during sliding is represented for each specimen type. The fitted points represent that two cycles took every 10,000 points, assumed to be exemplificative of the total evolution during the test. The *X*-axis plots the acquisition points, corresponding to the time progress, in a logarithmic scale. In Figure 7a the aluminium case is shown, and the cycles are quite irregular; this unpredicted behaviour, in the first analysis, can be attributed to an inhomogeneous specimen density in the proximity of the centre line of the stroke. In Figure 7b, the force evolution cycles for the titanium plate are shown. Again, the force has an irregular gait, but exhibits the typical hysteresis shape typical of this evolution. It has two peaks along the two central axes, where the ball diverts its motion and, consequently, the friction switches from the kinetic to the static phase. The loop cycles of the last two instances, namely the titanium coating (Figure 7c) and the laser-treated coating (Figure 7d), are outlined by a smooth hysteresis. These cycles exhibit a regular and flat shape during the sliding of the ball, i.e., the kinetic phase. The values of the energy ratio evaluated all along the test confirmed that the gross slip regime (wear-dominated regime) is always greater than 0.2, i.e., from a minimum of 0.3 to the maximum 0.9.

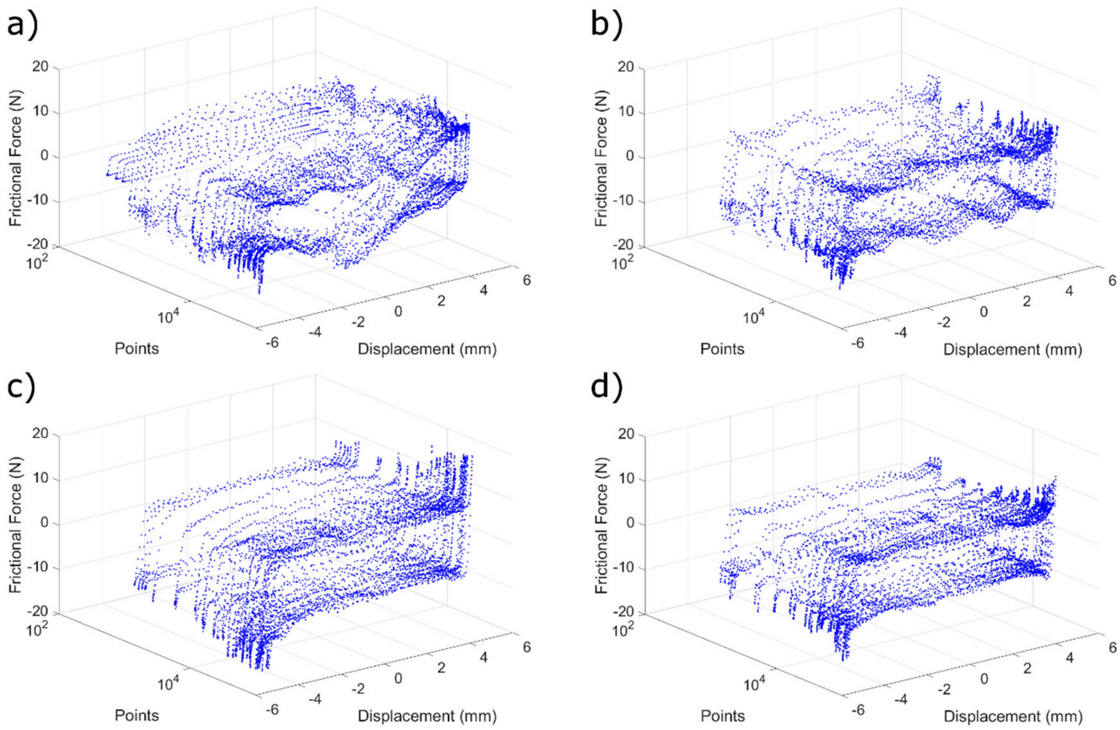

Figure 7. Loop cycles of the frictional force for: (**a**) aluminium; (**b**) titanium plate; (**c**) titanium coating; (**d**) laser-treated coating cases.

In Figure 8, the images obtained from the topography acquisitions are displayed. The wear track on the aluminium plate (Figure 8a) displays an uneven shape: it is non-symmetrical in respect to the *Y*-axis (perpendicular to the sliding direction). This observation is congruent with the friction loop cycles, which also exhibited irregular profiles. The wear track is deeper in proximity to the right central test-axis where the frictional force was the highest: the maximum wear depth along this midline profile is equal to 470 µm—the deepest recorded among the specimens. The titanium plate also exhibits an irregular shape (Figure 8b), with the deepest wear in the proximity of the two central axes of the ball—120 µm for the left and 130 µm for the right. It is also noticeable, as red points on the contour image, that there is an area of strong plastic deformation along the border of the wear track. In Figure 8c, the worn track of the titanium coating is displayed, and the profile is regular and smooth, presenting a maximum wear of 251 µm. This confirmed the poor resistance of cold spray coating against the counter-sphere, which results in a higher weight loss of the coating itself compared to both the titanium plate and oxidised layer (see Figure 6). Figure 8d shows the topography images on the laser-treated coating worn surface. As expected, the topography did not provide an unequivocal estimation of the wear depth, due to the irregular profile produced by the laser operation. As a result, the surface has an indented profile and the worn area is only distinguishable due to the presence of a large boundary incision.

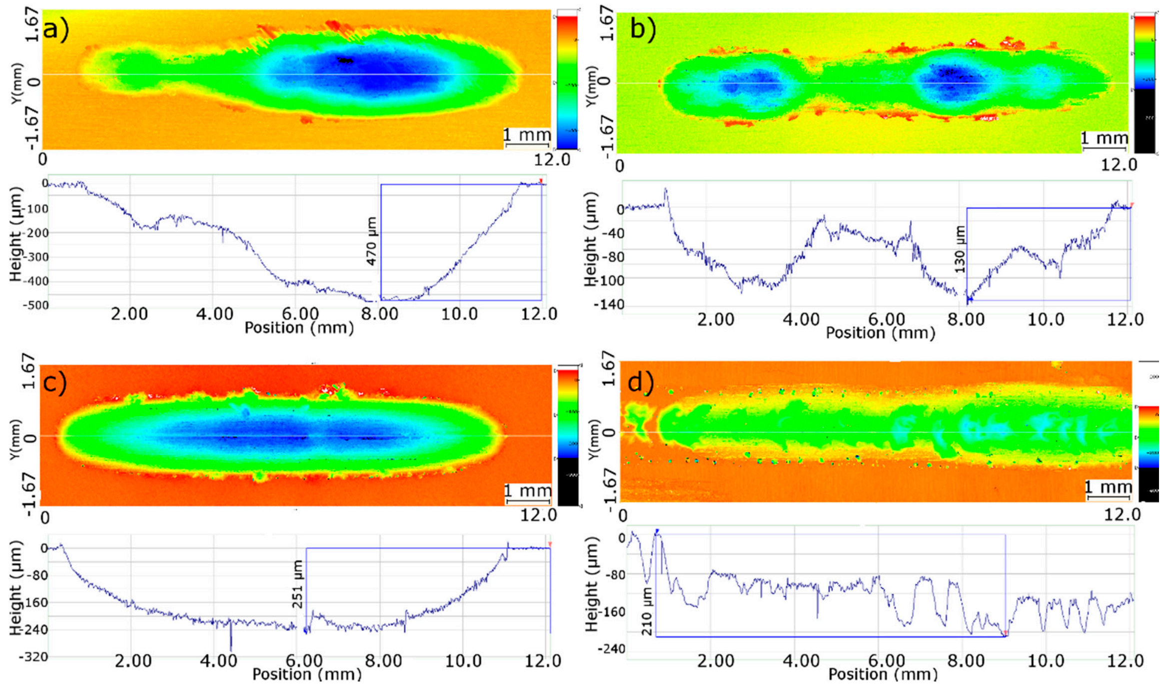

Figure 8. Wear tracks: contours and midline profiles: (**a**) aluminium plate; (**b**) titanium plate; (**c**) as-sprayed titanium coating; (**d**) laser-treated titanium coating.

4. Conclusions

The above presented and discussed results are summarised as follows. Both coatings under investigation, the treated one and the untreated one, showed better wear performances relative to the untreated AA2024 alloy. In particular the laser-treated coating showed the best wear resistance, better than the bulk titanium. These enhanced properties can be attributed to the presence of a superficial hard oxidised layer produced by the laser treatment. The presence of this oxide layer was confirmed by the EDX analysis in which an increase in the oxygen content within the treated area was observed. Three different metallurgical zones, with different microstructures, were visible in the areas of the treated tracks: the base material, the heat-affected zone and the treated zone. On the other hand, the temper state of the aluminium substrate was not affected by the process. The laser treatment influenced both the friction coefficient and the wear mechanism of the coating. The untreated coating showed an adhesive wear with a noticeable mass loss from the coating itself and a negligible wear of the ball. Abrasive wear mechanisms were observed testing the treated coating, with a negligible wear of the coating but a severe wear and mass lost on the sphere.

Acknowledgments: The authors gratefully thank Dermot Brabazon of the School of Mechanical and Manufacturing Engineering of the Dublin City University for the fruitful discussion concerning laser processing and treatments.

Author Contributions: All the authors contributed equally to this research activity. In particular: Claudio Leone and Silvio Genna carried out the laser treatment; Alessandro Ruggiero and Massimiliano Merola carried out the tribological tests; Antonello Astarita and Antonino Squillace carried out the cold spray deposition and also did some experimental tests; Pierpaolo Carlone and Felice Rubino carried out the experimental characterization. All the authors contributed at the writing of the paper.

Conflicts of Interest: The authors declare no conflict of interest.

References

1. Schmidt, T.; Gaertner, F.; Kreye, H. New Developments in Cold Spray Based on Higher Gas and Particle Temperatures. *J. Therm. Spray Technol.* **2006**, *15*, 488–494. [CrossRef]
2. Morgan, R.; Fox, P.; Pattison, J.; Sutcliffe, C.; O'Neill, W. Analysis of cold gas dynamically sprayed aluminium deposits. *Mater. Lett.* **2004**, *58*, 1317–1320. [CrossRef]
3. Marrocco, T.; McCartney, D.; Shipway, P.; Sturgeon, A. Production of titanium deposits by cold-gas dynamic spray: Numerical modeling and experimental characterization. *J. Therm. Spray Technol.* **2006**, *15*, 263–272. [CrossRef]
4. Astarita, A.; Durante, M.; Langella, A.; Montuori, M.; Squillace, A. Mechanical characterization of low pressure cold-sprayed metal coatings on aluminium. *Surf. Interface Anal.* **2013**, *45*, 1530–1535. [CrossRef]
5. Irissou, E.; Legoux, J.G.; Arsenault, B.; Moreau, C. Investigation of Al-Al_2O_3 Cold Spray Coating Formation and Properties. *J. Therm. Spray Technol.* **2007**, *16*, 661–668. [CrossRef]
6. Bell, T.; Dong, H. Enhanced wear resistance of titanium surfaces by a new thermal oxidation treatment. *Wear* **2000**, *238*, 131–137.
7. Wang, Y.; Li, C.; Guo, L.; Tian, W. Laser remelting of plasma sprayed nanostructured Al_2O_3-TiO_2 coatings at different laser power. *Surf. Coat. Technol.* **2010**, *204*, 3559–3566. [CrossRef]
8. Sidhu, B.S. Laser surface remelting to improve the erosion-corrosion resistance of nickel-chromium-aluminium-yttrium (NiCrAlY) plasma spray coatings. In *Laser Surface Modifications of Alloys for Corrosion and Erosion Resistance*; Kwok, C.T., Ed.; Woodhead Publishing: Cambridge, UK, 2012; pp. 355–366.
9. Chikarakara, E.; Aqida, S.; Brabazon, D.; Naher, S.; Picas, J.A.; Punset, M.; Forn, A. Surface modification of HVOF thermal sprayed WC-CoCr coatings by laser treatment. *Int. J. Mater. Form.* **2010**, *3*, 801–804. [CrossRef]
10. Chikarakara, E.; Naher, S.; Brabazon, D. High speed laser surface modification of Ti-6Al-4V. *Surf. Coat. Technol.* **2012**, *206*, 3223–3229. [CrossRef]
11. Chikarakara, E.; Naher, S.; Brabazon, D. Process mapping of laser surface modification of AISI 316L stainless steel for biomedical applications. *Appl. Phys. A Mater. Sci. Process.* **2010**, *101*, 367–371. [CrossRef]
12. Rubino, F.; Astarita, A.; Carlone, P.; Genna, S.; Leone, C.; Minutolo, F.M.C.; Squillace, A. Selective Laser Post-Treatment on Titanium Cold Spray Coatings. *Mater. Manuf. Process.* **2015**. [CrossRef]
13. Zhang, E.; Xu, L.; Yang, K. Formation by ion plating of Ti-coating on pure Mg for biomedical applications. *Scr. Mater.* **2005**, *53*, 523–527. [CrossRef]
14. Zhang, X.H.; Liu, D.X.; Tan, H.B.; Wang, X.F. Effect of TiN/Ti composite coating and shot peening on fretting fatigue behaviour of TC17 alloy at 350 °C. *Surf. Coat. Technol.* **2009**, *203*, 2315–2321. [CrossRef]
15. Qu, J.; Blau, P.J.; Watkins, T.R.; Cavin, O.B.; Kulkarni, N.S. Friction and wear of titanium alloys sliding against metal, polymer, and ceramic counterfaces. *Wear* **2005**, *258*, 1348–1356. [CrossRef]
16. Nieslony, P.; Cichosz, P.; Krolczyk, G.M.; Legutko, S.; Smyczek, D.; Kolodziej, M. Experimental studies of the cutting force and surface morphology of explosively clad Ti-steel plates. *Measurement* **2016**, *78*, 129–137. [CrossRef]
17. Ruggiero, A.; D'Amato, R.; Gómez, E.; Merola, M. Experimental comparison on tribological pairs UHMWPE/TIAL6V4 alloy, UHMWPE/AISI316L austenitic stainless and UHMWPE/Al_2O_3 ceramic, under dry and lubricated conditions. *Tribol. Int.* **2016**, *96*, 349–360. [CrossRef]
18. Ruggiero, A.; D'Amato, R.; Gómez, E. Experimental analysis of tribological behaviour of UHMWPE against AISI420C and against TiAl6V4 alloy under dry and lubricated conditions. *Tribol. Int.* **2015**, *92*, 154–161. [CrossRef]
19. Bloyce, A.; Morton, P.H.; Bell, T. *ASM Handbook*; ASM Int.: Materials Park, OH, USA, 1994; Volume 5, p. 835.
20. Bell, T.; Dong, H. Tribological enhancement of titanium alloys. In Proceedings of the First Asian Conference on Tribology, Beijing, China, 12–15 October 1998; pp. 421–427.
21. Dong, H.; Bell, T. Towards designer surfaces for titanium components. *Ind. Lubr. Tribol.* **1998**, *50*, 282–289. [CrossRef]
22. Friction, Lubrication, and Wear Technology. In *ASM Handbook*; Blau, P.J., Ed.; ASM Int.: Materials Park, OH, USA, 1994; Volume 18, p. 1879.
23. Astarita, A.; Durante, M.; Langella, A.; Squillace, A. Elevation of tribological properties of alloy Ti-6% Al-4%V upon formation of a rutile layer on the surface. *Met. Sci. Heat Treat.* **2013**, *54*, 662–666. [CrossRef]

24. Kataria, S.; Kumar, N.; Dash, S.; Tyagi, A.K. Tribological and deformation behaviour of titanium coating under different sliding contact conditions. *Wear* **2010**, *269*, 797–803. [CrossRef]
25. Khun, N.W.; Li, R.T.; Loke, K.; Khor, K.A. Effects of Al-Cr-Fe Quasicrystal Content on Tribological Properties of Cold-Sprayed Titanium Composite Coatings. *Tribol. Trans.* **2015**, *58*, 616–624. [CrossRef]
26. Cassar, G.; Wilson, J.C.A.-B.; Banfield, S.; Housden, J.; Matthews, A.; Leyland, A. Surface modification of Ti-6Al-4V alloys using triode plasma oxidation treatments. *Surf. Coat. Technol.* **2012**, *206*, 4553–4561. [CrossRef]
27. Wang, S.; Liao, Z.; Liu, Y.; Liu, W. Influence of thermal oxidation duration on the microstructure and fretting wear behaviour of Ti6Al4V alloy. *Mater. Chem. Phys.* **2015**, *159*, 139–151. [CrossRef]
28. Davis, J.R. (Ed.) *ASM Specialty Handbook: Aluminium and Aluminium Alloys*; ASM Int.: Materials Park, OH, USA, 1993.
29. Hanson, B. *The Selection and Use of Titanium: A Design Guide*; Institute of Materials: London, UK, 1995.
30. Ruggiero, A.; Valasek, P.; Merola, M. Friction and Wear Behaviours of Al/Epoxy Composites during Reciprocating Sliding Tests. *Manuf. Technol.* **2015**, *15*, 684–689.
31. Ruggiero, A.; Merola, M.; Carlone, P.; Archodoulaki, V.-M. Tribo-mechanical characterization of reinforced epoxy resin under dry and lubricated contact conditions. *Compos. B Eng.* **2015**, *79*, 595–603. [CrossRef]
32. Carlone, P.; Astarita, A.; Rubino, F.; Pasquino, N.; Aprea, P. Selective Laser Treatment on Cold-Sprayed Titanium Coatings: Numerical Modeling and Experimental Analysis. *Metall. Mater. Trans. B* **2016**. [CrossRef]
33. Wong, W.; Rezaeian, A.; Irissou, E.; Legoux, J.-G.; Yue, S. Cold Spray Characteristics of Commercially Pure Ti and Ti-6Al-4V. *Adv. Mater. Res.* **2010**, *89–91*, 639–644. [CrossRef]
34. Cassar, G.; Wilson, J.C.A.-B.; Banfield, S.; Housden, J.; Matthews, A.; Leyland, A. A study of the reciprocating-sliding wear performance of plasma surface treated titanium alloy. *Wear* **2010**, *269*, 60–70. [CrossRef]
35. Miller, P.D.; Holladay, J.W. Friction and Wear Properties of Titanium. *Wear* **1958**, *2*, 133–140. [CrossRef]
36. Budinski, K.G. Tribological properties of titanium alloys. *Wear* **1991**, *151*, 203–217. [CrossRef]
37. Krishna, D.S.R.; Brama, Y.L.; Sun, Y.R. Thick rutile layer on titanium for tribological applications. *Tribol. Int.* **2007**, *40*, 329–334. [CrossRef]
38. Dalili, N.; Edrisy, A.; Farokhzadeh, K.; Li, J.; Lo, J.; Riahi, A.R. Improving the wear resistance of Ti-6Al-4V/TiC composites through thermal oxidation (TO). *Wear* **2010**, *269*, 590–601. [CrossRef]
39. Kim, K.; Geringer, J. Analysis of energy dissipation in fretting corrosion experiments with materials used as hip prosthesis. *Wear* **2012**, *296*, 497–503. [CrossRef]
40. Fouvry, S.; Kapsa, P.; Vincent, L. Analysis of sliding behaviour for fretting loadings: Determination of transition criteria. *Wear* **1995**, *185*, 35–46. [CrossRef]
41. Sun, Y. Thermally oxidised titanium coating on aluminium alloy for enhanced corrosion resistance. *Mater. Lett.* **2004**, *58*, 2635–2639. [CrossRef]
42. Sun, Y. Tribological rutile-TiO_2 coating on aluminium alloy. *Appl. Surf. Sci.* **2004**, *233*, 328–335. [CrossRef]